Article

Journal of
Nanoscience and Nanotechnology
Vol. 17, 335–340, 2017
www.aspbs.com/jnn

Effects of MgO Nanocrystal Powder on Long-Term Sustain and Address Discharge Characteristics in ac-Plasma Display Panel

Jae Hyun Kim[1], Choon-Sang Park[2], Hyung Dal Park[3], Bhum Jae Shin[4], and Heung-Sik Tae[2,*]

[1] *Radiation Instrumentation Research Division, Korea Atomic Energy Research Institute, Daejeon 305-353, Republic of Korea*
[2] *School of Electronics Engineering, College of IT Engineering, Kyungpook National University, Daegu 702-701, Republic of Korea*
[3] *Department of Mechanical Equipment Development, Radiation Technology eXcellence (RTX), Daejeon 305-500, Republic of Korea*
[4] *Department of Electronics Engineering, Sejong University, Seoul 143-747, Republic of Korea*

We investigated the characteristics of MgO surface with MgO nanocrystal powders due to the long-term (500 hours) ion bombardment comparing with the conventional MgO surface in this study. When the MgO nanocrystal powders were coated on the conventional MgO surface, it was observed that the sputtered Mg particles from MgO surface were re-deposited on the MgO nanocrystal powders, which was able to significantly suppress the re-crystallization on the phosphor layers. We confirm that the MgO nanocrystal powders play a significant role in suppressing the degradation of the MgO surface and phosphor layer after long-term severe ion bombardments. Accordingly, when the MgO nanocrystal powers were applied to the conventional MgO surface, the variations of discharge characteristics, such as address discharge delay time, firing voltage of sustain and address discharge, and luminance, were significantly reduced comparing with the conventional MgO surface.

Keywords: MgO Surface, MgO Crystal Powder, Long-Term Discharge Characteristics, Plasma Application, Plasma Display Panel.

1. INTRODUCTION

The creation of new materials always provide the technological developments. Significant categories of materials in present technologies are represented by nanomaterials, nanostructures, and combinations of these.[1–3] The MgO nanocrystal powder has been introduced as a functional layer to improve the statistical delay time using an exo-emission in ac-plasma display panels (PDPs). It contributes to improving the electron emission in the shallow electron trap level below conduction band, i.e., exo-emission, which is not shown in the conventional MgO surface.[4–6] We recently reported the effects of the MgO nanocrystal powders on the discharge characteristics related to the panel temperature.[7] In the previous work, when the nano-MgO was coated on the MgO surface, the statistical delay characteristics were improved considerably especially under the low panel temperature.[7]

Despite a low sputtering yield of the MgO, degradation of the MgO surface would seem to be unavoidable due to ion bombardment. Therefore, the discharge characteristics, such as firing voltage, discharge delay time, and luminance, are also changed, especially in the case of long-term discharges. In the conventional MgO surface, it is reported that the address discharge delay time is increased because the electron emissions of the degraded MgO surface are deteriorated with an increase in the discharge time.[8–10] The firing voltage of sustain discharge is increased, while the firing voltage of address discharge is decreased. The former is manly related to the degradation of MgO surface, while the latter is manly related to the re-crystallization between the sputtered Mg particles and phosphor layer.[11,12] However, in the case of MgO surface with MgO nanocrystal powders, the influences of the sputtering phenomenon induced by long-term ion bombardments on the discharge characteristics have not fully investigated yet.

*Author to whom correspondence should be addressed.

This paper investigated the characteristics of the MgO surface coated by MgO nanocrystal powders relative to severe ion bombardments due to long-term (500 hours) discharges. In order to examine the effects of MgO nanocrystal powders on the variation of discharge characteristics, the firing voltage, address delay time, and luminance were monitored in the 42-inch PDP test panel with a high Xe content of 17% as a function of the discharge time from 0 to 500 hours. In addition, the scanning electron microscope (SEM), photoluminance (PL), and cathodoluminescence (CL) were carried out in order to investigate the morphology changes of the MgO surface and phosphor layers.

2. EXPERIMENTAL DETAILS

In this experiment, two 42-inch HD-grade panels were used as test panels, which specifications of two test panels were exactly the same except the MgO surface with and without MgO nanocrystal powders. The cell structure was a reflective 3-electrode surface discharge type of ac-PDP, as shown in Figure 1(a), where the transparent conductive electrodes with a bus electrode, common electrode (X) and scan electrode (Y), were responsible for the sustain discharge, while the address electrode (A) was responsible for the address discharge. The detailed specifications of the test panels are shown in Table I.

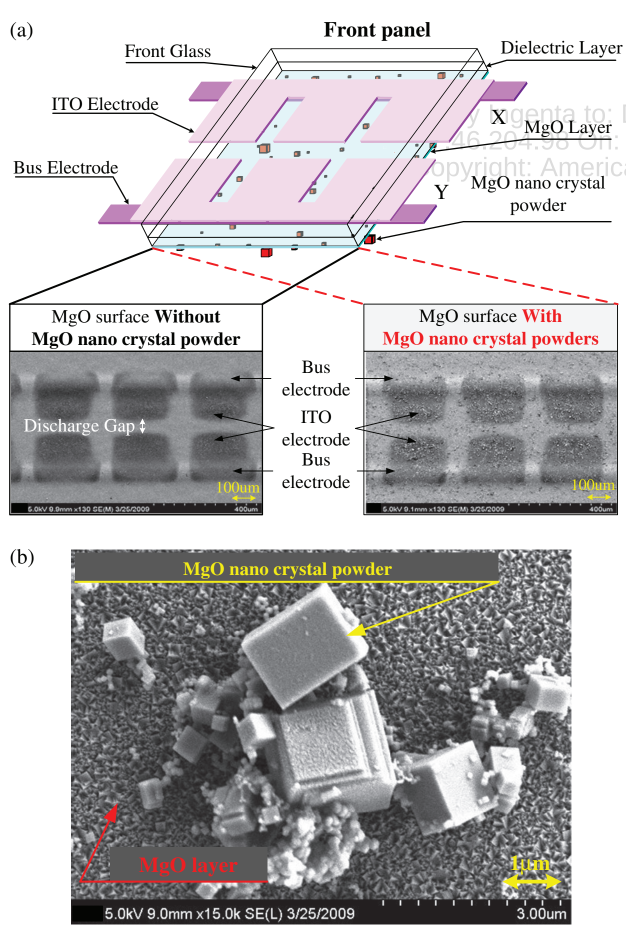

Figure 1. (a) SEM images of MgO surface without and with MgO nanocrystal powders in front panels of 42-inch HD-grade panels, and (b) enlarged SEM image of MgO nanocrystal powders on MgO surface.

Figure 1(a) also shows the SEM images of MgO surface with and without MgO nanocrystal powders in the front panels. In both cases, the MgO thin films were deposited on the dielectric layer using the ion-plating evaporation,[13] whereas the MgO nanocrystal powers (3 wt%) were coated on the MgO surface by using the spray method.[14] The addition of fluorine into the MgO nanocrystal powder was able to form the electron trap level below the conduction band in the band gap of MgO, such that it was possible to easily emit electrons in the discharge space. The grain size of the nano MgO with cubic type structure ranged from tens of nanometers to a few micrometers, as shown in Figure 1(b).

Figure 2 shows a schematic diagram of the experimental setup employed in this study. A pattern generator and logic signal generator were used to generate the conventional driving waveforms which were continuously applied to the test image pattern.[7,15] The square-type test image pattern occupied 1% of the entire display region of the 42-inch test panel, as shown in Figure 2. Plus, a color analyzer (CA-100 plus) and photo-sensor amplifier (Hamamatsu, C6386) were used to measure the luminance and IR emissions. To investigate the effects of the MgO nanocrystal powders due to the long-time ion bombardments, the test image pattern was continuously displayed from 0 to 500 hours by using the conventional waveform including the reset, address, and sustain period.[7,15,16] The frequency for the sustain period was 200 kHz. The same driving waveform voltage level was applied to both test panels, where the sustain voltage was 205 V.

3. RESULTS AND DISCUSSION

Figures 3(a and b) show the SEM images for both cases, i.e., with and without MgO nanocrystal powders, in order to investigate the morphology changes of the MgO surface after 500-hour discharge time in three regions: non-discharge region, discharge region near the bus electrode, and discharge region near the ITO electrode. As shown in Figure 3(a), grains with pyramidal morphologies were

Table I. Specifications of 42-in. HD test panel used in this study.

Front panel		Rear panel	
ITO width	225 μm	Barrier rib width	55 μm
ITO gap	70 μm	Barrier rib height	120 μm
Bus width	50 μm	Address width	95 μm
Cell pitch		912×693 μm	
Barrier rib type		Closed rib	
42-in.	Gas pressure	420 Torr	
	Gas chemistry	He (60%)–Ne–Xe (17%)	

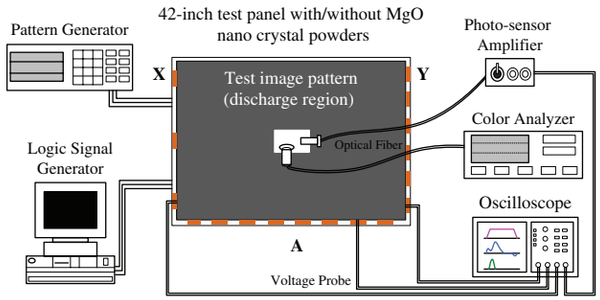

Figure 2. Schematic diagram of experimental setup employed in this study.

clearly found in the non-discharge region, whereas these pyramidal morphologies were destroyed in the discharge regions. In particular, severe destruction of the pyramidal morphologies was found near the ITO electrode, implying that the ion bombardment was more severe in the vicinity of the ITO electrode rather than the bus electrode. Meanwhile, as shown in Figure 3(b), MgO nanocrystal powders were founded to still remain on the MgO surface after 500-hour discharge time, confirming that the MgO nanocrystal powders were not eliminated by long-term ion bombardments. It should be noted that the Mg particles sputtered from the MgO surface were clearly observed to be re-deposited on the MgO nanocrystal powders. It would also affect the re-crystallization between the sputtered Mg particles and phosphor layer, which will be described later.

It is well-known that the address discharge delay time is closely related to the electron emission characteristics of the MgO surface. As such, the MgO degradation induced by ion bombardments during a long-time discharge aggravates the electron emission from the MgO surface, thereby resulting in increasing considerably the address discharge delay time relating to electron emission of the MgO surface. As previously described, the MgO nanocrystal powders play a significant role in reducing a statistical address discharge delay time caused by electron emissions in the sallow electron trap level. To investigate the variations of electron emission characteristics of the MgO nanocrystal powders induced by the severe ion bombardment during a long-term discharge, the changes in the address delay times were measured, as shown in Figure 4. As shown in Figures 4(a and b), for both cases, i.e., with and without MgO nanocrystal powders, the formative and statistical delay time were increased as increasing the discharge time. However, it was noted that the increment of statistical address discharge delay time due to ion bombardments was reduced when the MgO nanocrystal powders were applied to the conventional MgO surface.

Figures 5(a and b) show the cathodoluminescence (CL) spectra of MgO surface for both cases, i.e., with and without MgO nanocrystal powders, before and after 500-hour discharge. In Figure 5, the peak below a wavelength of 500 nm is mainly related to the emission capability of the electrons trapped from the F/F+ center, i.e., the secondary

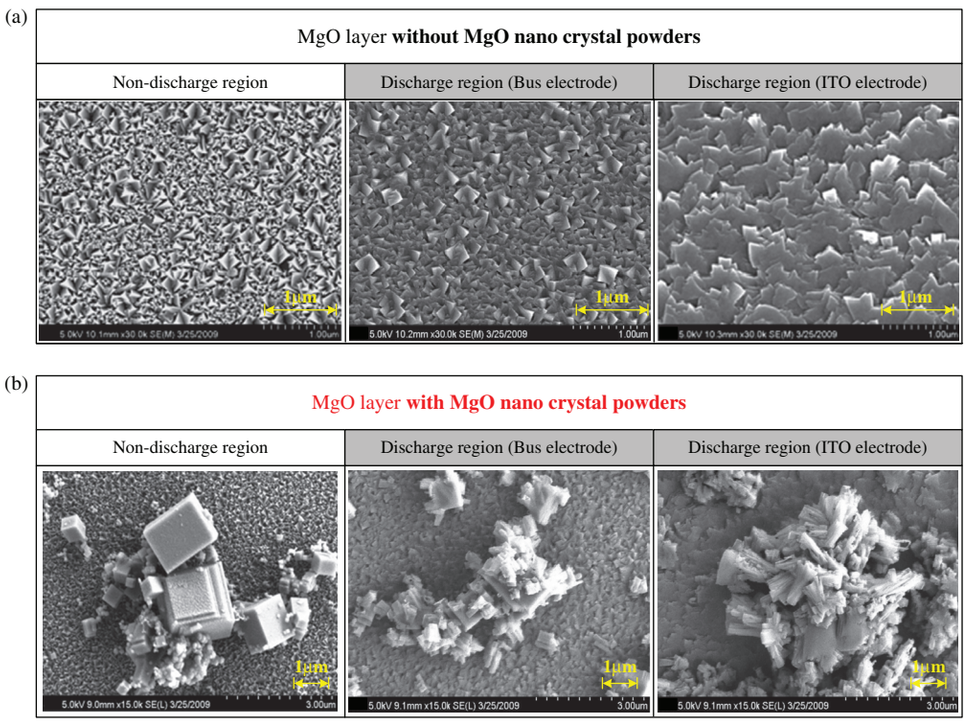

Figure 3. Comparison of SEM images of MgO surfaces (a) without and (b) with MgO nanocrystal powders after 500-hour discharge in three regions; non-discharge region, discharge region near bus electrode, and discharge region near ITO electrode.

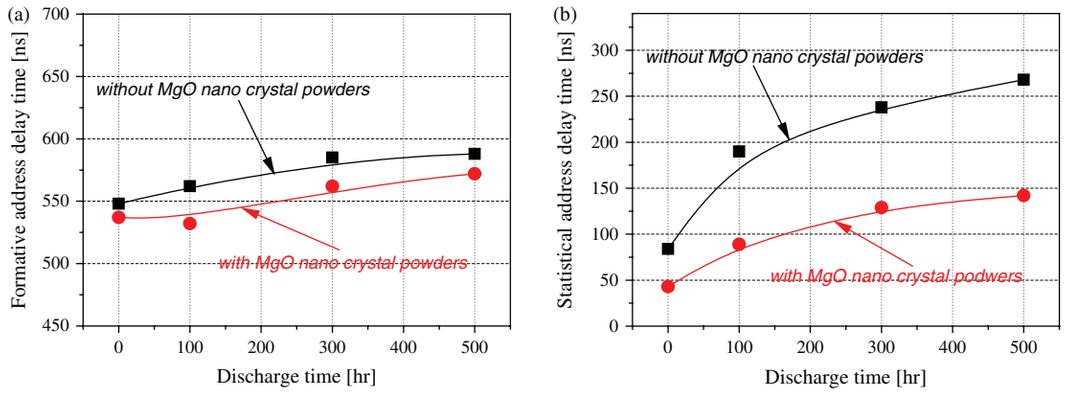

Figure 4. Comparison of (a) formative and (b) statistical address delay time measured from discharge region relative to discharge time for MgO surfaces without and with MgO nanocrystal powders.

electron emission, whereas the other shallow peak above a wavelength of 600 nm is mainly related to the emission capability of the electrons trapped by the low energy level of the MgO surface, i.e., the exo-emission.[17, 18] For both cases, the F/F+ center and shallow emission peaks of the MgO surfaces were decreased, as shown in Figures 5(a and b). However, the intensity of CL was less decreased when the MgO nanocrystal powders were coated on the MgO surface. Therefore, we can infer that the MgO nanocrystal powders would mitigate the degradation of the MgO surface due to the ion bombardments.

Figure 6(a) shows the variations of the firing voltage between the *X–Y* electrodes for both cases, i.e., with and without MgO nanocrystal powders, after 500-hour discharge time. The firing voltage was increased in both cases, which was mainly related to the degraded MgO

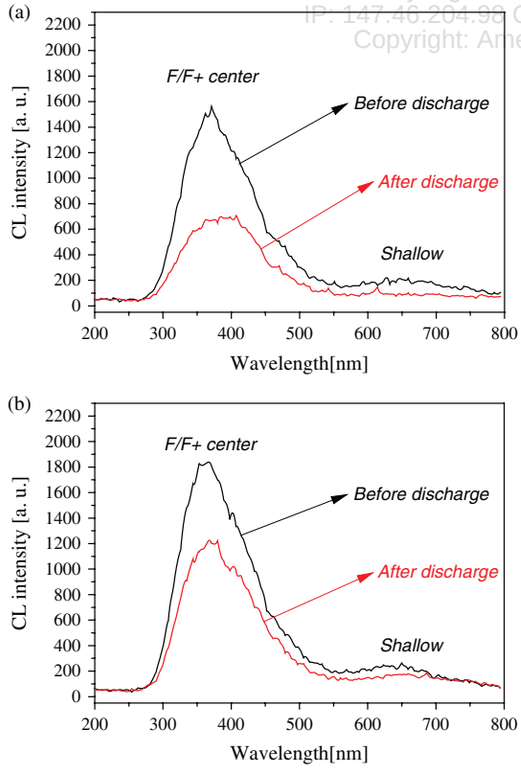

Figure 5. Comparison of cathodoluminescence (CL) spectra of MgO surface (a) without and (b) with MgO nanocrystal powders before and after 500-hour discharge.

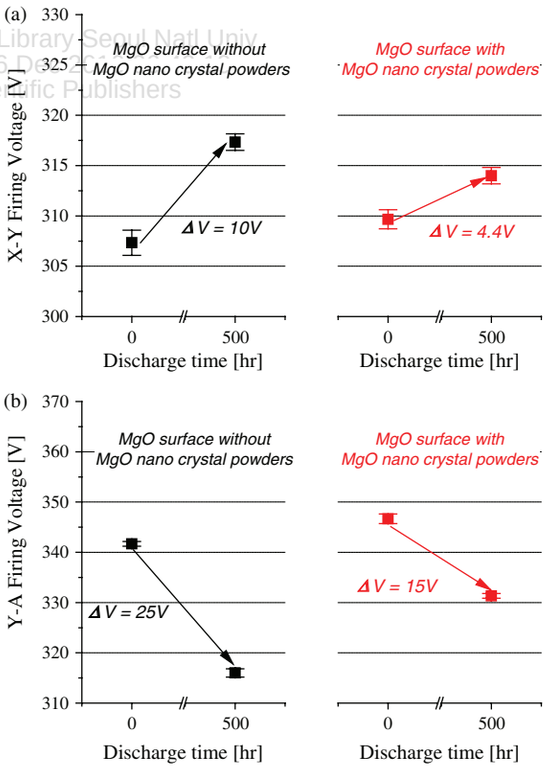

Figure 6. Changes in firing voltages measured from discharge region relative to discharge time for both cases, i.e., with and without MgO nanocrystal powders; (a) firing voltage between *X–Y* electrodes under MgO cathode condition and (b) firing voltage between *Y–A* electrodes under phosphor cathode condition.

surface due to ion bombardments. However, as shown in Figure 6(a), the variation of the firing voltage between the X–Y electrodes ($=\Delta V_{fxy}$) for the MgO surface with MgO nanocrystal powders was smaller than that for the conventional MgO surface, indicating that the MgO nanocrystal powders played a role in suppressing the degradation of the MgO surface. Figure 6(b) shows the variation of the firing voltage between the Y–A electrodes ($=V_{fya}$) where the V_{fya} means that the firing voltage between the scan electrode and the address electrode when the address electrode is acted as a cathode. As previously described, the V_{fya} was decreased in both cases. Since the V_{fya} was strongly related to phosphor properties, we could infer that the decrease in the V_{fya} was mainly due to re-crystallization between the sputtered Mg particles and the phosphor layer.[11, 12, 19] However, as shown in Figure 6(b), the ΔV_{fya} of the MgO surface with MgO nanocrystal powders was much smaller than that for the conventional MgO surface. The suppression in re-crystallization between the sputtered Mg particles and phosphor layer might be mainly related to the re-deposition on the MgO nanocrystal powders, as shown in Figure 3(b).

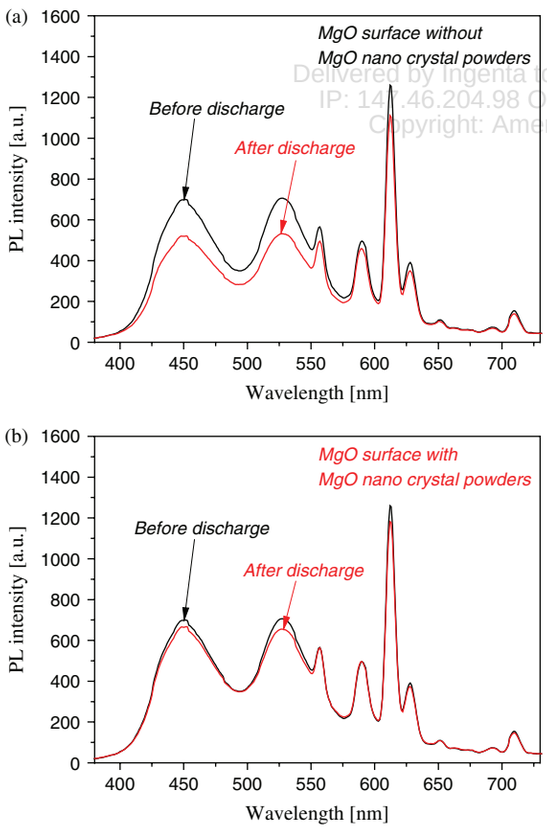

Figure 7. Comparison of profiles of photo intensity (172 nm using Kr lamp) based on PL analysis of phosphor layer before and after 500-hour discharge for MgO surfaces (a) without and (b) with MgO nanocrystal powders.

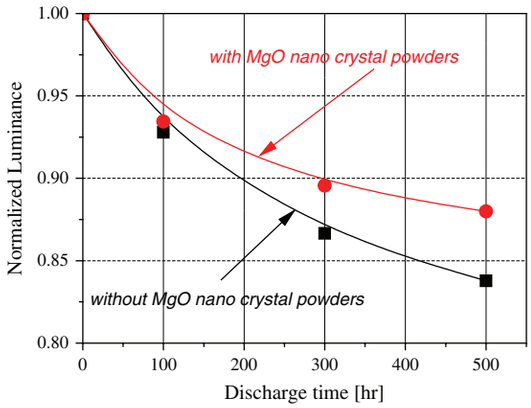

Figure 8. Changes in normalized luminance relative to discharge time for both cases, i.e., with and without MgO nanocrystal powders.

Figures 7(a and b) show the photoluminance (PL) spectra measured from the phosphor layers for both cases, i.e., with and without MgO nanocrystal powders, when using a Kr vacuum ultra-violet lamp (172 nm) to irradiate the red, green, and blue phosphor layers before and after the 500-hour discharge. As shown in Figure 7(a), the intensity of PL was observed to be significantly decreased, which also indicated that the phosphor layer was degraded due to the re-crystallization between the sputtered Mg particles and the phosphor layers. On the contrary, it should be noted that the intensity of PL is slightly decreased when the MgO nanocrystal powders are coated on the MgO surface, as shown in Figure 7(b). Therefore, we can confirm that the MgO nanocrystal powders play a significant role in suppressing the re-crystallization between the sputtered Mg particles and the phosphor layer.

Figure 8 shows the changes in the normalized luminance for both cases, i.e., with and without MgO nanocrystal powders relative to the discharge time. The normalized luminance was defined as the luminance difference ratio between the initial luminance and the luminance at a certain discharge time in the discharge region, as shown in Eq. (1).

$$L_n = 1 - \left(\frac{L_i - L_c}{L_i} \right) \tag{1}$$

In Eq. (1), L_n, L_i, and L_c are the normalized luminance, initial luminance, and luminance at a certain discharge time, respectively. As shown in Figure 8, the normalized luminance of the MgO surface with and without MgO nanocrystal powders was decreased as increasing the discharge time, which noted that the decrement of luminance was significantly reduced when the MgO nanocrystal powders were applied to the conventional MgO surface.

4. CONCLUSIONS

We investigates the characteristics of MgO surface with MgO nanocrystal powders due to the long-term (500 hours) ion bombardment comparing with the

conventional MgO surface in this study. When the MgO nanocrystal powders are coated on the conventional MgO surface, the sputtered Mg particles from MgO surface are observed to be re-deposited on the MgO nanocrystal powders. Furthermore, it helps to decrease the re-crystallization on the phosphor layers, which confirms that the MgO nanocrystal powders play a significant role in suppressing the degradation of the MgO surface and phosphor layer after long-term severe ion bombardments. Accordingly, when the MgO nanocrystal powders are coated on the MgO surface, the changes of firing voltages, i.e., the ΔV_{fxy} and ΔV_{fya}, are significantly reduced comparing the conventional MgO surface. Furthermore the changes in the address delay time as well as the luminance are also decreased.

Acknowledgments: This research was supported by Basic Science Research Program through the National Research Foundation of Korea (NRF) funded by the Ministry of Education (NRF-2013R1A1A4A03008577).

References and Notes

1. D. Jariwala, V. K. Sangwan, L. J. Lauhon, T. J. Marks, and M. C. Hersam, *ACS Nano* 8, 1102 **(2014)**.
2. K. Ariga, Y. Yamauchi, G. Rydzek, Q. Ji, Y. Yonamine, K. C.-W. Wu, and J. P. Hill, *Chem. Lett.* 43, 36 **(2014)**.
3. J. Yao and H. Wang, *Chem. Soc. Rev.* 43, 4470 **(2014)**.
4. T. Okada, T. Naoi, and T. Yoshioka, *J. Appl. Phys.* 105, 113304 **(2009)**.
5. J. S. Choi, S. H. Moon, J. H. Kim, and G. H. Kim, *Curr. Appl. Phys.* 10, 1378 **(2010)**.
6. T. Naoi, H. Lin, A. Hirota, E. Otani, and K. Amemiya, *J. Soc. Inf. Disp.* 17, 113 **(2009)**.
7. J. H. Kim, C.-S. Park, H. D. Park, H.-S. Tae, and S.-H. Lee, *J. Nanosci. Nanotechnol.* 13, 3270 **(2012)**.
8. S. J. Yoon and I. S. Lee, *J. Appl. Phys.* 91, 2487 **(2002)**.
9. C.-S. Park, J. H. Kim, S.-K. Jang, H.-S. Tae, and E.-Y. Jung, *J. Soc. Inf. Disp.* 18, 606 **(2010)**.
10. G.-S. Kim and S.-H. Lee, *IEEE Trans. Plasma Sci.* 39, 1470 **(2011)**.
11. C.-S. Park, H.-S. Tae, and S.-I. Chien, *Appl. Phys. Lett.* 99, 083503 **(2011)**.
12. C. H. Ha, J. S. Kim, D. C. Jeong, and K. W. Whang, *J. Appl. Phys.* 96, 4807 **(2004)**.
13. G. S. Lee, K. B. Kim, J. J. Kim, and S. H. Sohn, *J. Phys. D: Appl. Phys.* 42, 105402 **(2009)**.
14. S.-M. Oh, J.-H. Byun, and Y.-G. Hwang, U.S. Patent 8303928 B2 **(2012)**.
15. J. P. Boeuf, *J. Phys. D: Appl. Phys.* 36, R53 **(2003)**.
16. K. Yoshikawa, Y. Kanazawa, and M. Wakitani, *Japan Display '92: Proceedings of the Twelfth International Display Research Conference*, International Conference Center Hiroshima, Hiroshima, Japan, October **(1992)**, p. 605.
17. C.-S. Park, H.-S. Tae, E.-Y. Jung, J. H. Seo, and B. J. Shin, *IEEE Trans. Plasma Sci.* 38, 2439 **(2010)**.
18. H. Tolner, *The 9th Asian Symposium on Information Display (ASID)*, New Delhi, India, October **(2006)**, p. 136, http://www.iitk.ac.in/asid06/proceedings/forms/introduction.htm.
19. C. H. Ha, B. Y. Han, J. S. Yoo, H. S. Bae, and K.-W. Whang, *J. Electrochem. Soc.* 155, J230 **(2008)**.

Received: 6 February 2015. Accepted: 23 September 2015.